J Mater Sci: Mater Med (2014) 25:173–183
DOI 10.1007/s10856-013-5059-2

Monetite and brushite coated magnesium: in vivo and in vitro models for degradation analysis

Shaylin Shadanbaz · Jemimah Walker · Tim B. F. Woodfield · Mark P. Staiger · George J. Dias

Received: 12 March 2013 / Accepted: 19 September 2013 / Published online: 1 October 2013

Abstract The use of magnesium (Mg) as a biodegradable metallic replacement of permanent orthopaedic materials is a current topic of interest and investigation. The appropriate biocompatibility, elastic modulus and mechanical properties of Mg recommend its suitability for bone fracture fixation. However, the degradation rates of Mg can be rapid and unpredictable resulting in mass hydrogen production and potential loss of mechanical integrity. Thus the application of calcium phosphate coatings has been considered as a means of improving the degradation properties of Mg. Brushite and monetite are utilized and their degradation properties (alongside uncoated Mg controls) are assessed in an in vivo subcutaneous environment and the findings compared to their in vitro degradation behaviour in immersion tests. The current findings suggest monetite coatings have significant degradation protective effects compared to brushite coatings in vivo. Furthermore, it is postulated that an in vitro immersion test may be used as a tentative predictor of in vivo subcutaneous degradation behavior of calcium phosphate coated and uncoated Mg.

S. Shadanbaz (✉) · J. Walker · G. J. Dias
Department of Anatomy, University of Otago, Dunedin, New Zealand
e-mail: shaylin.shadanbaz@anatomy.otago.ac.nz

T. B. F. Woodfield
Department of Orthopaedic Surgery and Musculoskeletal Medicine, University of Otago, Christchurch, New Zealand

M. P. Staiger
Department of Mechanical Engineering, University of Canterbury, Christchurch, New Zealand

1 Introduction

Magnesium (Mg) is a lightweight metal suggested for investigations as a degradable replacement for current permanent metallics used for orthopaedic applications [1–10]. Mg demonstrates, not only biocompatibility, but also the ability to promote osteogenesis and exhibits an elastic modulus closer to that of human bone compared to titanium and stainless-steel [11–15]. Subsequently, Mg offers the advantage of sufficient mechanical integrity for bone fixation and immobilization in fracture management, whilst mitigating stress shielding, and the requirements of a second surgery for implant removal associated with permanent devices.

Mg degrades via the following equation (overall)

$$Mg^{+} + 2H_2O \leftrightarrow Mg(OH)_2 + H_{2(gas)}$$

In an aqueous environment, Mg corrodes and develops a thin Mg hydroxide film on its surface, which creates a poor passivation layer, and gaseous hydrogen as a by product [16]. In an in vivo environment, excess hydrogen causes gas pocket formation, and the resulting hydroxide ions (OH^{-}) cause an increase in alkalinity in surrounding tissue [17]; both of which have been shown to retard healing [18]. Thus, whilst the degradation properties of Mg are advantageous, the corrosion rate must be closely controlled to minimise hydrogen gas production [18, 19] and avoid premature mechanical failure [20–24] to allow effective bone healing.

Calcium phosphate coatings have long been utilised as a means of increasing the biocompatibility of permanent metals in orthopaedic use owing to their natural occurrence in several biological structures, including teeth and bone [25, 26]. Different calcium phosphate phases not only have different solubility co-efficients and biocompatibility

properties depending on environmental conditions (including pH, temperature and environmental composition), but also often require different synthesis protocols [3]. Calcium phosphate coating technologies used in recent research include, but are not limited to, sol–gel protocols [27–29], electrodeposition [30–32], biomimetic techniques [33–35] and plasma spraying [36–38]. These protocols frequently focus on titanium substrates and concentrate on improving the biocompatibility of the substrate [39–42]. More recently, the use of calcium phosphates and their coating technologies have been used to address and improve the corrosion properties of degradable metals [11, 43–46].

The suggestion of calcium phosphates as a corrosion resistant coating for Mg requires the development of a coating technology that will not affect the surface integrity of the substrate, whilst providing effective adherence and transient protection of the substrate. In previous studies, we developed an alternative and novel immersion coating protocol, which has been successfully used for the application of brushite (dicalcium phosphate dehydrate) and monetite (dicalcium phosphate anhydrous) calcium phosphate bioceramic coatings to reduce and control the rate of corrosion on Mg substrates in vitro [47]. Brushite is a precursor to the more stable and insoluble hydroxyapatite (HA) [48–50] with a relatively low solubility coefficient compared to most calcium phosphates [51–53]. Furthermore, thermal hydrolysis results in conversion to monetite and may be promoted by the presence of Mg ions which can disrupt brushite crystal formation favouring conversion to monetite [54]. In turn, monetite is capable of converting to HA under favourable conditions also including in vivo scenarios [3, 54, 55]. Literature further suggests monetite to exhibit lower passive and active degradation when compared to brushite in in vitro corrosion studies [56]. Whereas, in vivo monetite ceramics exhibit faster resorption rates compared to brushite, as seen when implanted in rabbit cortical bone over 4 weeks period [57]. This same phenomenon is observed in vivo (as in the current study), with monetite obtained by the conversion of brushite using hydrothermal processes [58].

Although the increased solubility of both brushite and monetite compared to insoluble HA suggests poor long-term corrosion resistance, we propose that the solubility will be adequate for controlled degradation of under-lying Mg substrates, whilst providing a source of calcium (Ca^{2+}) and phosphate (HPO_4^-) ions for enhanced osteogenicity. Osteoclastic activity in vivo has shown Ca^{2+} and HPO_4^- release from the bone matrix which has in turn demonstrated significant effects on bone cell proliferation and differentiation [59]. Furthermore, Ca^{2+} (intracellular and extracellular) has been identified as essential in complex processes such as bone remodeling acting as a chemotactic signal for pre-osteoblasts to the required bony site as well as influence the maturation of the cells [60–63]. In vitro investigations have also shown the effects of extracellular Ca^{2+} to be concentration-dependent where concentrations higher than physiological levels are favoured [64–66]. HPO_4 on the other hand has been shown to regulate cell cycle, proliferation rates and the secretion of bone related proteins [67]. Thus, to reiterate, it is postulated that the use of soluble calcium phosphates will improve bony response when compared to insoluble HA.

The aim of this study was to assess the corrosion behavior of these two calcium phosphate phases, brushite and monetite, in a highly vascular location compared to an uncoated substrate. The coatings tested here are intended for application on Mg based orthopaedic implants, necessitating their eventual investigation in an intraosseous environment. However, intraosseous surgical procedures commonly require the use of large animals, and thus complex and costly operations [68]. Additionally, with biodegradable materials such as Mg, it would be unethical to implant an actively corroding material in a hard tissue environment without fully characterizing the likely in vivo response [68]. Thus this major leap from in vitro testing to intraosseous testing suggests that there is a requirement for an intermediate investigative step [68]. For these reasons, a subcutaneous study in rats was implemented to assess the corrosion and biocompatibility of the materials in vivo prior to intraosseous studies. The intention would be to use these findings as a tentative predictor of corrosion in an intraosseous environment. The selection of a subcutaneous location was due to its vascularity and large area of soft tissue available in this layer. This ensured a physiologically dynamic site for corrosion rate estimation, and for the effective assessment of tissue response. One of the benefits of this highly vascular location is rapid access by inflammatory mediators. This would ensure that the corrosion of implants observed here is not underestimated for future intraosseous experiments. Additionally, utilising a subcutaneous location allows one to maximize the implantation of a large number of samples per animal [68].

The use of gravimetric analysis allowed us to determine the most corrosion resistant coating. This study also allowed us to compare in vivo subcutaneous corrosion rates to in vitro immersion tests [47] to determine reliable screening strategies for future Mg corrosion analysis and improved in vivo experimental design.

2 Materials and methods

All reagents reported herein were obtained from Sigma-Aldrich, Missouri, USA.

2.1 Sample preparation

Pure Mg (obtained from Timmenco Ltd., Toronto, Canada, 99.99 %) was machined to rectangular blocks (12 mm × 4 mm × 3 mm), polished to 1,000 grit and coated with brushite and monetite. The coating technique used was an immersion technique where a series of temperature and time controlled steps were utilized to grow a calcium phosphates, from a calcium phosphate solution, onto the surface of the Mg as described previously [47]. In brief, samples were pre-treated via immersion in NaOH and then transferred to a calcium phosphate bath for either 120 min at 50 °C to obtain brushite or a 2 step incubation was performed where samples were incubated for 60 min at 60 °C followed by incubation in fresh solution for 90 min at 85 °C to obtain monetite. Electron dispersive spectroscopy (EDS, JEOL 2300F EDS, Tokyo, Japan) was performed as well as glancing angle X-ray diffraction (GA-XRD) to confirm the presence and identity of the coatings. GA-XRD was performed on an X'Pert Pro PANaltyical, Almelo, Netherlands) with a Cu anode. The glancing angle was maintained at 5° while scans were performed at 3°–80°. The temperature remained constant at 20 °C throughout the analysis. X'Pert Data Collector (version 2.0e, PANalytical, Almelo, Netherlands) was used for XRD data collection. A combination of X'Pert HighScore Plus (version 2.2e, PANalytical, Almelo, Netherlands) and a Joint-Committee-on-Powder-Diffraction-Spectra (JCPDS) database was used to analyse the spectra. Spectral background manipulations and peaks were identified using automatic algorithms with X'Pert HighScore Plus software (PANalytical, Almelo, Netherlands).

2.2 In vitro immersion testing

The in vitro immersion technique was performed as described in Shadanbaz et al. [47]. Briefly, all samples (coated and uncoated) were weighed and sterilised with UV radiation prior to immersion in simulated body fluid (SBF). The size of the samples and solution volumes were selected to mimic the approximate size of a large orthopaedic implant in the human. All samples were immersed in either 30 mL of Earle's Balanced Salt solution (EBSS), Minimum Essential Media (MEM), or MEM with 40 g/L of bovine serum albumin (MEM-P) [to mimic blood plasma concentrations] and buffered with physiological sodium bicarbonate system (2.2 g/L, 26 mmol). The experiment was carried out in T-25 cell culture flasks under dynamic conditions using an orbital shaking platform at 300 rev/min (IKA® Vibrax, VXR basic, Selangor, Malaysia) in a 37 °C and a 5 % CO2 environment for 7, 21 and 28 days respectively. Daily, 14 mL of media was replaced to mimic physiological urinary excretion [69]. Post immersion, samples were removed and cleaned in a chromic acid solution (200 g/L CrO_3 and 10 g/L $AgNO_3$). Preliminary experiments assessing the corrosion product removal protocol indicated that all dissolution occurring was specific to the corrosion products on the surface of the Mg. Gravimetric analysis was performed using GraphPad Prism (version 5.0 for Mac OS X, GraphPad Software, San Diego California USA, www.graphpad.com) and findings are presented graphically.

2.3 In vivo analysis

All in vivo testing was carried out in accordance with institutional animal ethics approval (University of Otago Animal Ethics Committee AEC 74/10). Lewis (inbred) rats were selected for this study to minimise any intra-species variation. A total of twelve mature male Lewis rats were used with 3 animals allocated to each time point 21, 42, 63 and 84, days. All samples were prepared as described above to be consistent, to enable accurate comparison between samples. Gamma irradiation (25–32 kGy) was used for sample sterilisation. Each animal received 6 implants (two uncoated, two brushite and two monetite) in a subcutaneous pocket on the dorsal abdominal region of the rat as shown in Fig. 1. A subcutaneous location was selected as a highly vascular in vivo location. This ensured a physiologically dynamic site for corrosion rate estimation. Consequently, the suitability of coated Mg as an implantable biomaterial may be determined using the current findings, before advancing to a more invasive surgery to test this material in a bony location. Sample allocation was determined systematically to remove location bias. All surgical protocols were carried out under aseptic conditions.

All animals received prophylactic antibiotics in the form of streptomycin (Southern Medical Products, Dunedin, NZ) subcutaneously, 30 min prior to surgery. Analgesia was provided 20 min pre-operatively and 24 h post-operatively via subcutaneous injection of non-steroidal anti-inflammatory carprofen (5 mg/kg, Southern Medical Products, Dunedin, NZ). Anaesthesia was induced using 4 % halothane:2 L/min oxygen after which anaesthesia was maintained at 2 % halothane:1 L/min oxygen. The dorsal aspect of the animal was shaved and disinfected using 70 % chlorhexidine gluconate. Six 5 mm bilateral skin incisions were made on the dorsal abdominal aspect of the rat and a subcutaneous pocket formed by blunt dissection to allow the insertion of the samples (Fig. 1). After implantation of the samples, incision sites were closed with a single interrupted suture (3/0, C7 needle, Monomend MT Monofilament, Veterinary Products Laboratories, Phoenix, USA) (Fig. 1). All animals were housed separately post-operatively. Hydrogen production, a consequence of Mg

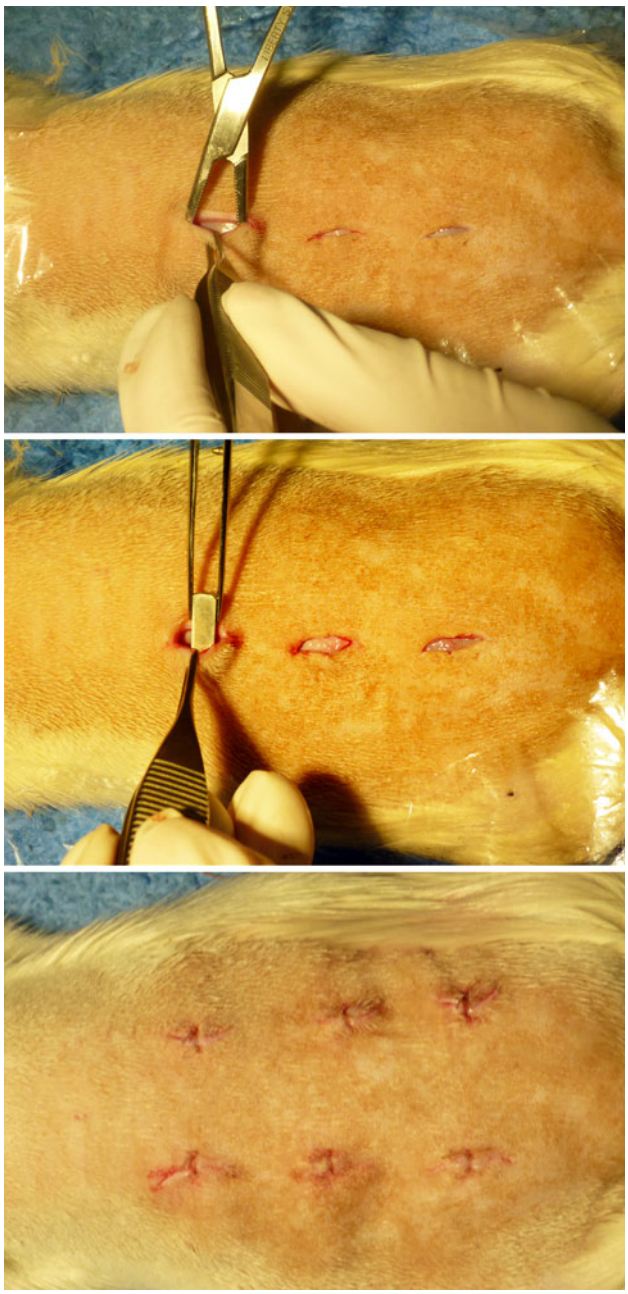

Fig. 1 (*Top*) Surgical image showing three of the six bilateral incisions created on the dorsal aspect of the rat using blunt dissection. (*Middle*) The first implant (uncoated) is being placed into the most rostral pocket of the three subcutaneous pockets shown. (*Bottom*) Incision sites were closed with a single interrupted suture as shown here

corrosion, was monitored by palpation and visual assessment. Presence of any hydrogen was also noted at the post mortem.

At days 21, 42, 63 and 84, animals were euthanized via CO_2 asphyxiation and samples harvested for analysis. Corrosion products were removed in a chromic acid solution as described in the in vitro protocol above.

2.4 Gravimetric examination, corrosion rates and statistical analyses

All gravimetric data was illustrated graphically comparing coated and uncoated corrosion performance, within in vitro and in vivo experiments, as well as between in vitro and in vivo experiments. Sample weights were measured post chromic acid cleaning (as described previously) and weight loss was calculated as a percentage difference from the original sample weight prior to coating. In vitro findings were analysed using a univariate generalised linear model with post hoc Bonferroni analysis for all immersion times (7, 21 and 28 days). Fixed variables were media and coating whilst weight loss was the dependent variable. In vivo gravimetric data was analysed with a generalised linear model with repeated measures with post hoc Bonferroni analysis for all implantation times (21, 42, 63, and 84 days). Gravimetric statistical analysis was performed using SPSS statistics software package (IBM SPSS Statistics, Version 19, Chicago, USA).

Corrosion rates of samples were calculated from gravimetric data according to the following formula:

$$CR = \frac{KW}{ATD}$$

where CR is the corrosion rate (mm/year), K is the constant 8.76×10^4, W is the mass loss (g), A is the surface area (cm^2), T is the time of exposure (h), and D is the density of the materials (g/cm^3) [70]. Corrosion data at matching time points between in vitro and in vivo experiments were statistically analysed using a one-way analysis of variance (ANOVA) with a Bonferroni post hoc test where in vivo was identified as the control group, using GraphPad Prism software (GraphPad Software, San Diego California USA).

3 Results

3.1 Characterization of coatings

All coatings were characterised and confirmed as brushite and monetite using scanning electron microscopy (SEM), EDS and GA-XRD (Fig. 2). This data can also be found in the paper published recently by the authors [47]. Both coatings appeared homogenous, porous, and crystalline in structure upon visual assessment (Fig. 2). Brushite comprises predominantly of large plate-like crystals (20–30 microns in length) whilst monetite is made up of primarily small crystal 'globules' (30–100 microns across consisting of smaller crystals: 5–20 microns). The brushite and monetite coatings on Mg surfaces are both rich in calcium and phosphate exhibiting average thicknesses of 43.65 ± 2.49 and 17.93 ± 2.03 μm, respectively (Fig. 2).

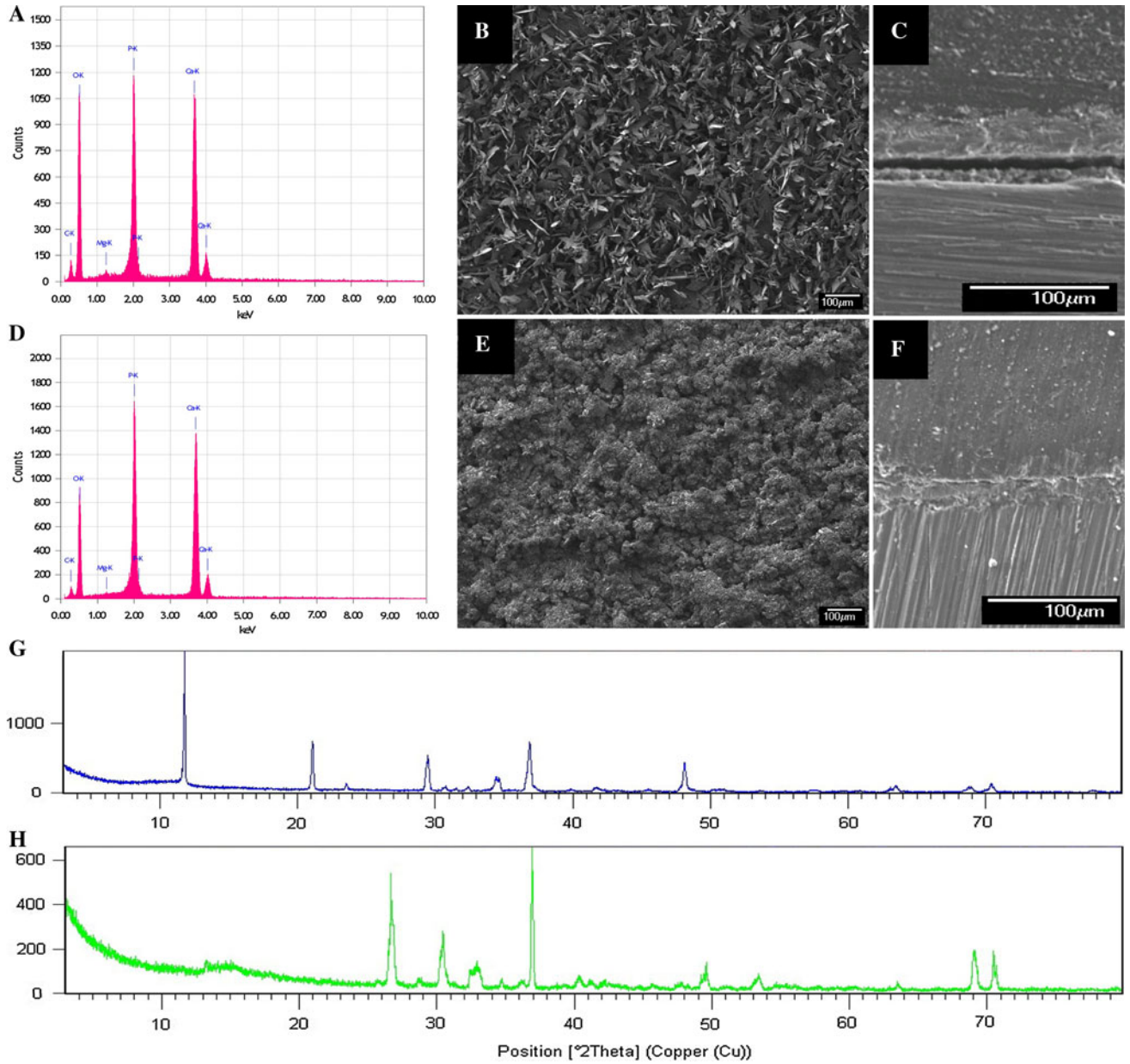

Fig. 2 EDS analysis of brushite (**a**) or monetite (**d**) coatings where the first, second and third major peaks represent oxygen, phosphorous, and calcium respectively. Typical SEM images are also included of the brushite (**b**) or monetite (**e**) coatings. Cross sectional analysis (adjacent) displaying the coating thickness of the brushite (**c**) or monetite (**f**) coating can be seen in the corresponding panels revealing an average thickness of 46.76 ± 1.29 μm for the biomimetic brushite, 43.65 ± 2.49 μm for brushite, and 17.93 ± 2.03 μm for the monetite. Glancing angle X-ray diffraction of the brushite coating (**g**) or monetite coating (**h**), units are displayed as intensity (counts/s)

3.2 In vitro gravimetric analysis

Gravimetric analysis of samples, after chromic acid cleaning, was recorded graphically as a percentage of their original (pre coating) mass (Fig. 3). Data was analysed using a univariate generalised linear model with post hoc Bonferroni analysis for all immersion times (7, 21 and 28 days). Whilst a corrosive protective trend of brushite was apparent in EBSS and MEM, there was no significant difference when compared to the uncoated control. Immersion of brushite coated Mg in MEM containing protein, demonstrated significant corrosion protection ($P < 0.0001$) across all time points when compared to the uncoated controls. Monetite coatings exhibited significant corrosion protective properties across all time points in EBSS ($P < 0.05$) and MEM containing protein ($P < 0.0001$). A protective trend was evident in MEM also. Monetite consistently displayed greater protective effects than brushite across all time points and solutions, however these observations were not statistically significant.

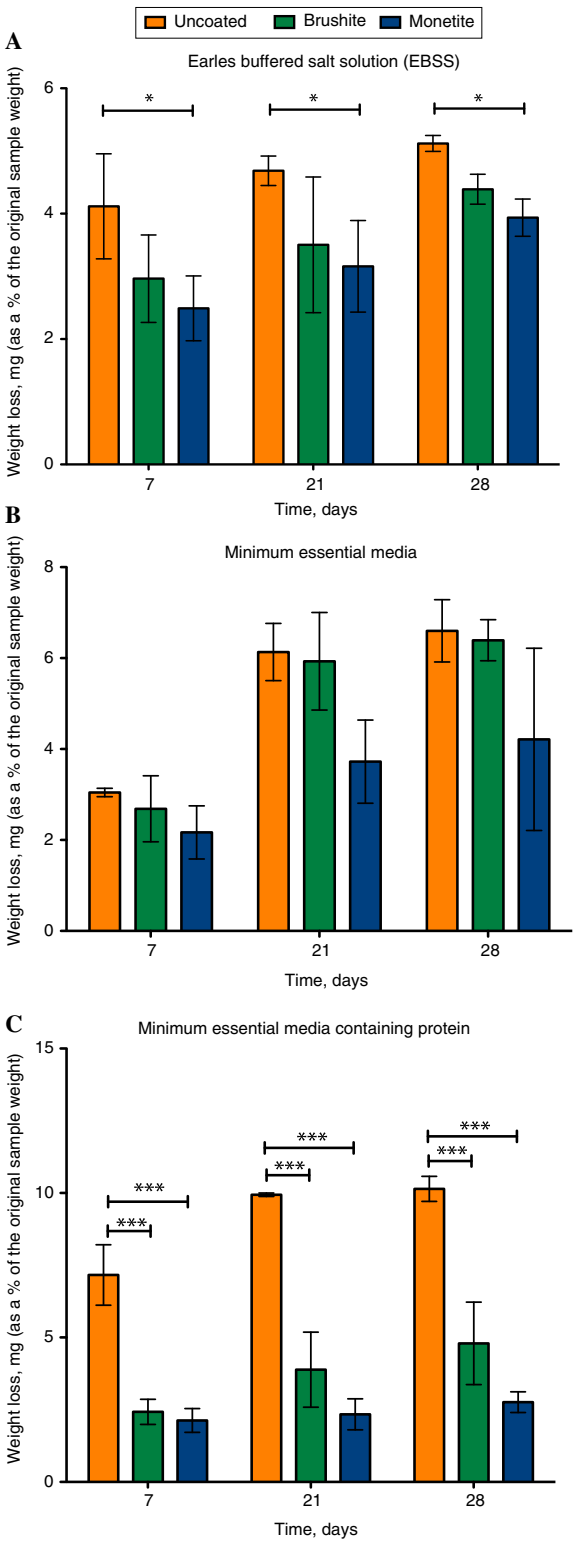

Fig. 3 The above graphs illustrate weight loss as a percentage of the original weight for uncoated and brushite or monetite coated samples where samples were immersed in either EBSS (**a**), MEM (**b**) or protein containing MEM (**c**). All data values are an average of the mean, $n = 3$. $^{***}P < 0.0001$, $^{*}P < 0.05$

3.3 In vivo corrosion morphology and tissue response

Clinically detectable hydrogen production was not encountered through palpation and visual assessment throughout the time points in any of the animals. Post mortem analysis supported these observations confirming minimal to no hydrogen production in proximity of the implants and implant sites. Hydrogen production was not observed around either brushite or monetite coated samples across all time points, although hydrogen bubbles within soft tissue were observed surrounding 5/24 of the uncoated Mg samples (Fig. 4). These bubbles were observed at the earlier 3 and 6 week time points with no evidence of hydrogen bubbles remaining by 9 and 12 weeks. Whilst not observed in all animals, post mortem analysis revealed occasional migration of implants within their subcutaneous pockets before anchoring in soft tissue (Fig. 5). Additionally, in contrast to the coated samples, corrosion was more pronounced on the surfaces of the uncoated Mg (Fig. 6) after 12 weeks.

3.4 In vivo gravimetric analysis

All samples remained in a subcutaneous location for 21, 42, 63, and 84 days after which animals were euthanised, samples removed, cleaned and assessed for gravimetric changes. All changes were recorded graphically as a percentage of their (pre coating) original weight (Fig. 7). Data was analysed with a generalised linear model with repeated measures with post hoc Bonferroni analysis for all implantation times (21, 42, 63, and 84 days). Reduced corrosion rates were observed in the brushite coated samples when compared to uncoated controls, ($P < 0.05$) over time. This decrease in corrosion closely followed the pattern of corrosion of the uncoated control over time as can be seen in Fig. 7. The monetite coated samples exhibited significantly reduced corrosion rates ($P < 0.004$) over time when compared to uncoated controls. No significant difference was seen in corrosion protection between the brushite and monetite coatings over the experimental 84-day period, although the latter demonstrated a greater corrosion protection trend.

3.5 In vitro versus in vivo corrosion rates

The matching time point of 21 days between in vitro and in vivo experiments was used to compare the corrosion rates of coated and uncoated Mg. This data was analysed using a one-way analysis of variance (ANOVA) with a Bonferroni post hoc test where in vivo was identified as the control group. No significant difference in corrosion

Fig. 4 Demonstrates established hydrogen bubbles surrounding an uncoated magnesium implant (*left*) compared to a coated magnesium implant (*right*) in a subcutaneous location at 3 weeks

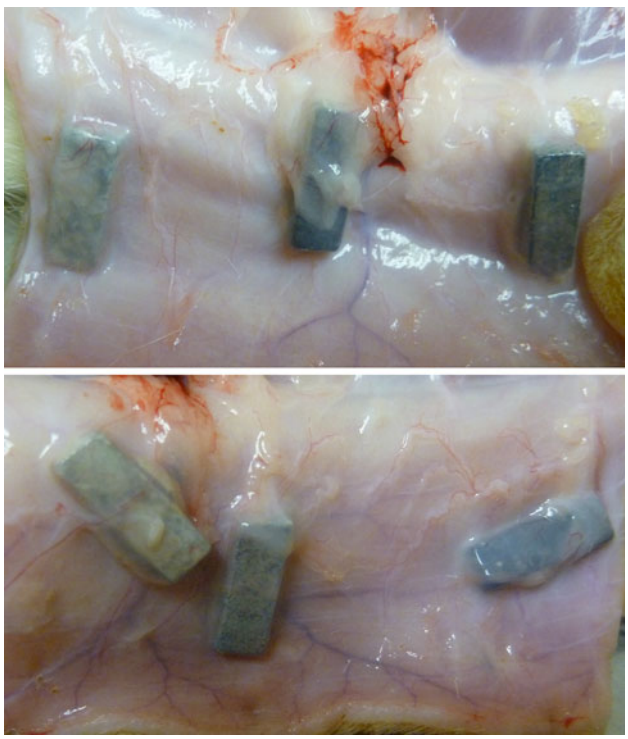

Fig. 5 The *top panels* shows the implant sites of the magnesium implants after successful anchoring in the subcutaneous fascia whilst the *lower panel* illustrates migration that occurred in the subcutaneous layer during the period of implantation

rate was observed between solution types at 21 days with either the brushite or the monetite coating (Fig. 8). However, significant differences ($P < 0.05$) were demonstrated in uncoated Mg samples between MEM/MEM containing protein and in vivo corrosion rates (Fig. 8). No

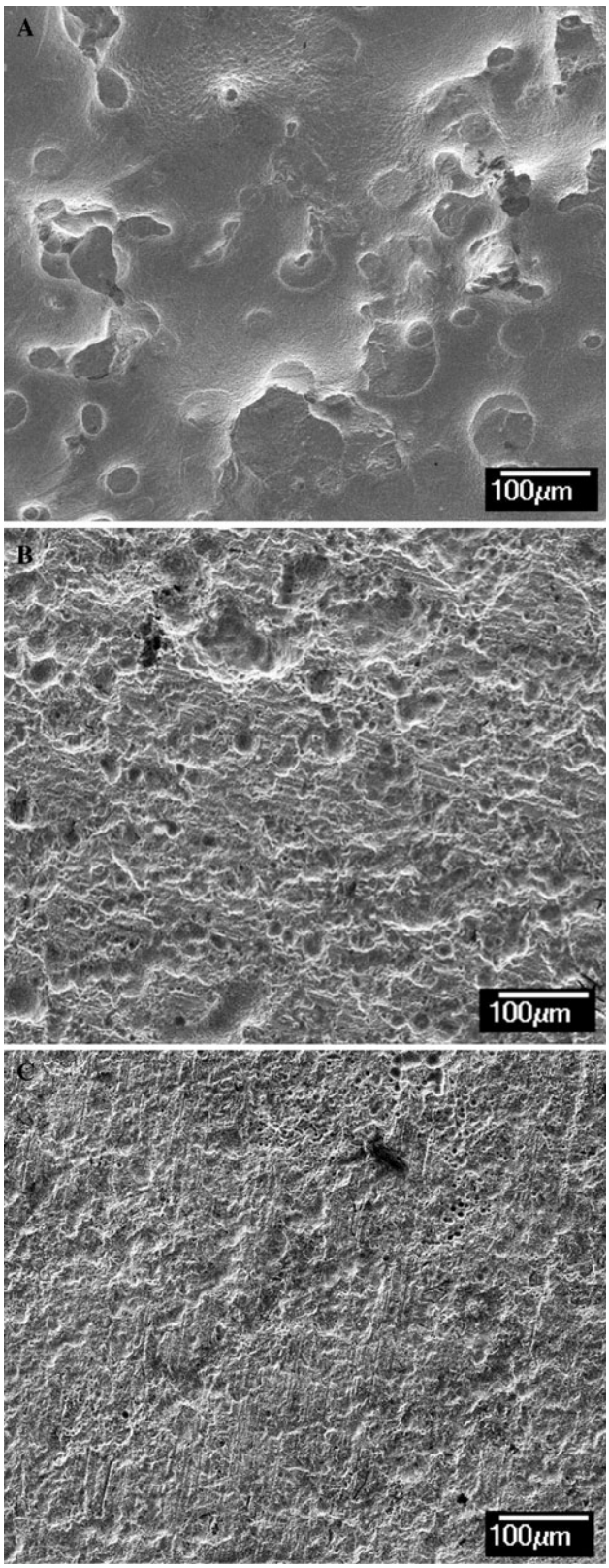

Fig. 6 SEM images of uncoated (**a**), brushite (**b**) and monetite (**c**) coated samples after cleaning with a chromic acid solution post 12-week implantation in subcutaneous tissue in rats

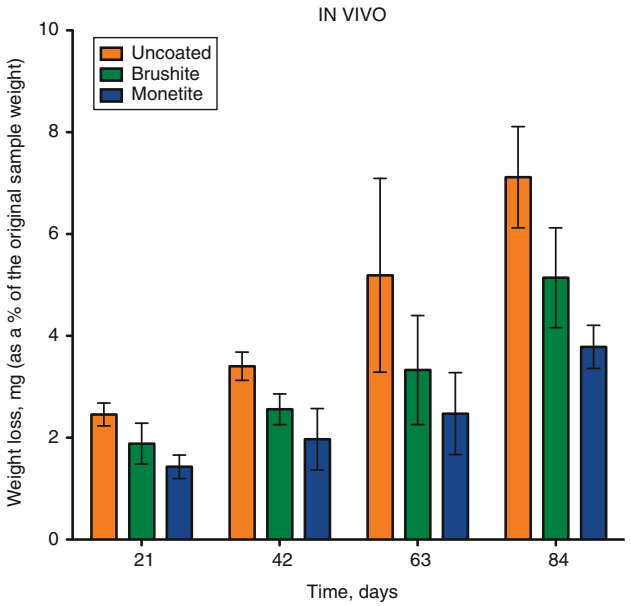

Fig. 7 The above graphs shows the gravimetric changes as a percentage of the original weight for uncoated and brushite or monetite coated samples where samples placed in a subcutaneous pocket on the dorsal region of the rat for 21, 42, 63 and 84 days. All data values are an average of the mean, $n = 6$. $^{**}P < 0.004$, $^{*}P < 0.05$

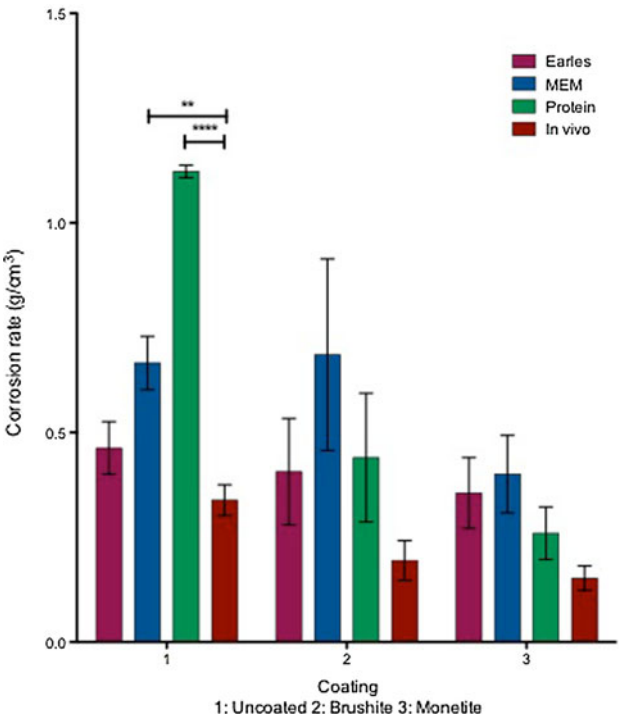

Fig. 8 Corrosion rate analysis indicating the different corrosion patterns observed with the coated and uncoated samples both in vivo and in vitro at the matching time point of 21 days. $^{****}P < 0.0001$, $^{**}P < 0.01$

difference was seen between EBSS and in vivo corrosion rates.

4 Discussion

In order to determine the suitability of various calcium phosphate coatings for controlling Mg corrosion, the calcium phosphates of interest must be investigated in both an in vitro and in vivo environment. This study confirms significantly improved corrosion resistance of calcium phosphate monetite phase coated Mg compared to brushite phase and uncoated Mg substrates in both in vitro and in vivo tests. Furthermore, we demonstrate EBSS to be the most accurate in vitro predictor of in vivo subcutaneous Mg corrosion rates (uncoated and coated).

Monetite and brushite calcium phosphates have, to date, been most commonly used in bone cements due to their similarity to biological apatites and osteoconductive/osteoinductive properties [71–73]. Furthermore, their bioresorption properties compared to insoluble HA make them promising candidates for retardation rather than complete elimination of Mg implant corrosion [3]. For the development of Mg as an orthopaedic biomaterial, it is necessary to control its corrosion so as to optimize and correctly balance the rate of implant degradation with subsequent new bone formation to promote optimal healing conditions. High corrosion rates can lead loss of mechanical and the possibility of premature implant failure, in additional to pathological hydrogen production and thus altered local pH in surrounding tissues [17, 74]. As reflected in the current investigation, the monetite coating demonstrated significant corrosion protection both in vitro and in vivo, whilst brushite showed significant protection in vitro and a protective trend in vivo compared to the uncoated control. Our findings are in agreement with recent literature that demonstrated monetite and brushite to have sufficient corrosion protection properties on Mg based on in vitro studies, with monetite showing a trend of superior corrosion protection [75–78]. Wang et al. [75] showed substantially lower corrosion of brushite coated Mg samples compared to uncoated samples in SBF. Similarly, Chun-Yan et al. [79] found Mg alloy coated with calcium phosphates to have significantly higher corrosion resistance compared to uncoated alloys in vitro. Li et al. [78] further showed brushite to demonstrate corrosion protection compared to uncoated samples. The authors also found heated treated brushite (forming monetite in a similar way to the monetite obtained within the current study) to provide additional corrosion resistance compared to brushite and uncoated samples. Conversely, alternative findings utilizing electrochemical impedance spectroscopy tests on brushite coated Mg have suggested the coating to be too thin and irregular in morphology to provide effective corrosion resistance long term [76].

Whilst other investigators have suggested improved properties by converting the brushite phase to a HA-like phase leading to increased corrosion resistance [80]. In view of the findings of the current study, we propose the monetite coating to have superior corrosion resistance to the brushite coating owing partly to its higher solubility coefficient at 37 °C and thus greater resistance to dissolution at this temperature [77]. Greater physical thickness of the coating has also been suggested by investigators to promote corrosive protective properties of calcium phosphates [81] in contrast to our study where the relatively thinner monetite coating outperformed the brushite coating. Recent investigations have postulated that monetite improves apatite deposition in vivo, and hence may result in enhanced thickness of protective coating and improved osteoconductivity [78]. Moreover, limited hydrogen production was seen in vivo particularly in the coated samples indicating decreased corrosion rates in the presence of calcium phosphate coatings. This ability to maintain hydrogen levels within physiological buffering capacity seen in this study is in accordance with recent publications [76].

Upon immediate assessment, in vitro corrosion rates appear to be higher than in vivo corrosion rates. However, these observations are only statistically significant between uncoated samples in MEM/MEM containing protein and in vivo test conditions. Surprisingly, these findings indicate EBSS, the simplest of the simulated body fluids, having the greatest potential for tentatively predicting the in vivo corrosion rates of calcium phosphate coated and uncoated Mg. Our observations corroborate those of Walker et al. [82] where corrosion of Mg alloys were consistently lowest in an in vivo subcutaneous location or an EBSS immersion when compared to MEM and protein containing MEM immersion tests. The data here further suggests that the two calcium phosphate coatings experience corrosion attack at more similar rates, than the uncoated samples, between the three solutions and subcutaneously in vivo. Thus speculating that in vitro testing for corrosion rates of uncoated Mg requires more consideration than coated Mg. In line with this, recent literature has demonstrated that the lowest corrosion rates for uncoated Mg can be seen in simpler solutions i.e. artificial seawater and PBS when compared to the more physiologically relevant and complex cell culture media such as Dulbecco's modified eagle medium (MEM) or Hanks solution (HBSS) [83, 84]. In contrast, Yamamoto et al. [69] indicated immersion of uncoated Mg in NaCl solution to result in substantially higher degradation when compared to the more physiologically relevant Earle's minimum essential media containing protein, whilst other investigators have likewise shown uncoated Mg in protein containing media to have similar corrosion patterns [85]. These discrepancies in corrosion rates in vitro, however, are most probably the consequence of inconsistent methodologies between investigators i.e. solution composition and volume, sample size, substrate impurities, static or dynamic conditions [46, 82, 86–89].

5 Conclusions

Using an in vivo subcutaneous location for Mg implantation, the current findings have illustrated that monetite coatings on Mg to have significant corrosion protection effects, whilst brushite coatings demonstrated only a protective trend. Additionally, we speculate that EBSS solution may be used as a tentative predictor of in vivo corrosion rates for both uncoated and calcium phosphate coated Mg samples. It is important to highlight however, that whilst these in vivo corrosion rates and coating behaviors are limited to a subcutaneous location, these findings allow the screening of possible candidates prior to advancement to more invasive and complex studies in large animals where bony locations may be investigated for both corrosion and biocompatibility.

References

1. Williams D. New interests in magnesium. Med Device Technol. 2006;17(3):9.
2. Brar HS, et al. Magnesium as a biodegradable and bioabsorbable material for medical implants. JOM. 2009;61(9):31–4.
3. Shadanbaz S, Dias GJ. Calcium phosphate coatings on magnesium alloys for biomedical applications: a review. Acta Biomater. 2011;8(1):20–30.
4. Salahshoor M, Guo Y. Surface integrity of biodegradable Magnesium-Calcium orthopedic implant by burnishing. J Mech Behav Biomed Mater. 2011;4(8):1888–904.
5. Hornberger H, Virtanen S, Boccaccini A. Biomedical coatings on magnesium alloys—a review. Acta Biomater. 2012;8(7):2442–55.
6. Manuel MV, Hort N. Magnesium: an essential nutrient for a good biomaterial. JOM. 2011;63(4):99.
7. Witte F. The history of biodegradable magnesium implants: a review. Acta Biomater. 2010;6(5):1680–92.
8. Malekani J et al. Biomaterials in orthopedic bone plates: a review. Glob Sci Technol Forum. 2011.
9. Persaud-Sharma D, McGoron A. Biodegradable magnesium alloys: a review of material development and applications. J Biomim Biomater Tissue Eng. 2012;12:25–39.
10. Wang J et al. Surface modification of magnesium alloys developed for bioabsorbable orthopedic implants: a general review. J Biomed Mater Res Part B Appl Biomater. 2012;100B(6):1691–701.
11. Chai H et al. In vitro and in vivo evaluations on osteogenesis and biodegradability of a β-tricalcium phosphate coated magnesium alloy. J Biomed Mater Res Part A 2011;100A(2):293–304.
12. Yang J et al. In vivo biocompatibility and degradation behavior of Mg alloy coated by calcium phosphate in a rabbit model. J Biomater Appl. 2011;27(2):153–64.
13. Zhao S et al. Effects of magnesium-substituted nanohydroxyapatite coating on implant osseointegration. Clin Oral Implants Res. 2011;24(A100):34–41.

14. Wagner DW, Lindsey DP, Beaupre GS. Deriving tissue density and elastic modulus from microCT bone scans. Bone 2011;49(5):931–38.
15. Zhou YL, et al. Compressive properties of hot-rolled Mg–Zr–Ca alloys for biomedical applications. Adv Mater Res. 2011;197:56–9.
16. Song GL, Atrens A. Corrosion mechanisms of magnesium alloys. Adv Eng Mater. 1999;1(1):11–33.
17. Gray Munro J, Seguin C, Strong M. Influence of surface modification on the in vitro corrosion rate of magnesium alloy AZ31. J Biomed Mater Res Part A. 2009;91(1):221–30.
18. Witte F, et al. In vivo corrosion of four magnesium alloys and the associated bone response. Biomaterials. 2005;26(17):3557–63.
19. Staiger M, et al. Magnesium and its alloys as orthopedic biomaterials: a review. Biomaterials. 2006;27(9):1728–34.
20. Kannan MB, Orr L. In vitro mechanical integrity of hydroxyapatite coated magnesium alloy. Biomed Mater. 2011;6:045003.
21. Witte F, et al. Degradable biomaterials based on magnesium corrosion. Curr Opin Solid State Mater Sci. 2008;12(5–6):63–72.
22. Xin Y, et al. Corrosion behavior of biomedical AZ91 magnesium alloy in simulated body fluids. J Mater Res. 2007;22(7):2004–11.
23. Groves EWH. An experimental study of the operative treatment of fractures. Br J Surg. 1913;1(3):438–501.
24. Gu XN, Zheng YF. A review on magnesium alloys as biodegradable materials. Front Mater Sci Chin. 2010;4(2):111–5.
25. Choi J, et al. Calcium phosphate coating of nickel-titanium shape-memory alloys. Coating procedure and adherence of leukocytes and platelets. Biomaterials. 2003;24(21):3689–96.
26. Hanawa T, Ota M. Calcium phosphate naturally formed on titanium in electrolyte solution. Biomaterials. 1991;12(8):767–74.
27. Qu J, et al. Silver/hydroxyapatite composite coatings on porous titanium surfaces by sol-gel method. J Biomed Mater Res B Appl Biomater. 2011;97(1):40–8.
28. Roy A et al. Novel sol–gel derived calcium phosphate coatings on Mg4Y alloy. Mater Sci Eng B 2011;176(20):1679–89.
29. Sureshbabu S, et al. Biomimetic deposition of hydroxyapatite on titanium with help of sol-gel grown calcium pyrophosphate prelayer. Mater Res Innov. 2011;15(3):178–84.
30. Chai YC et al. Perfusion electrodeposition of calcium phosphate on additive manufactured titanium scaffolds for bone engineering. Acta Biomater. 2011;7(5):2310–19.
31. Drevet R, et al. In vitro dissolution and corrosion study of calcium phosphate coatings elaborated by pulsed electrodeposition current on Ti6Al4V substrate. J Mater Sci Mater Med. 2011;22(4):753–61.
32. Lin DY, Wang XX. Preparation of hydroxyapatite coating on smooth implant surface by electrodeposition. Ceram Int. 2011;37(1):403–6.
33. Elkoca O, et al. Hydroxyapatite coating on Cp–Ti implants by biomimetic method. Adv Mater Res. 2012;445:679–84.
34. Dressler M et al. Sol–gel preparation of calcium titanium phosphate: viscosity, thermal properties and solubility. J Sol–Gel Sci Technol 2012:1–8.
35. Karakas A, et al. Yttria-doped zirconia-hydroxyapatite composite coating on Cp–Ti implants by biomimetic method. Adv Mater Res. 2012;445:691–6.
36. Robotti P, Zappini G. Thermal plasma spray deposition of titanium and hydroxyapatite on polyaryletheretherketone implants. PEEK Biomater Handb 2011:119.
37. Singh G, Singh S, Prakash S. Surface characterization of plasma sprayed pure and reinforced hydroxyapatite coating on Ti6Al4V alloy. Surf Coat Technol. 2011;205(20):4814–20.
38. Demnati I et al. Hydroxyapatite coating on titanium by a low energy plasma spraying mini-gun. Surf Coat Technol. 2011;206(8–9):2346–53.
39. Yang F et al. Osteoblast response to puerarin-loaded porous titanium surfaces: an in vitro study. J Biomed Mater Res Part A. 2012;100A(6):1419–26
40. Alghamdi HS et al. Biological response to titanium implants coated with nanocrystals calcium phosphate or type 1 collagen in a dog model. Clin Oral Implants Res. 2012;24(5):475–83.
41. Palarie V et al. Early outcome of an implant system with a resorbable adhesive calcium–phosphate coating—a prospective clinical study in partially dentate patients. Clin Oral Invest 2011:1–10.
42. Fontana F, et al. Effects of a calcium phosphate coating on the osseointegration of endosseous implants in a rabbit model. Clin Oral Implant Res. 2011;22(7):760–6.
43. Jo JH et al. Hydroxyapatite coating on magnesium with MgF 2 interlayer for enhanced corrosion resistance and biocompatibility. J Mater Sci Mater Med. 2011:1–11.
44. Waterman J, et al. Improving in vitro corrosion resistance of biomimetic calcium phosphate coatings for Mg substrates using calcium hydroxide layer. Corros Eng Sci Technol. 2012;47(5):340–5.
45. Tomozawa M, Hiromoto S. Growth mechanism of hydroxyapatite-coatings formed on pure magnesium and corrosion behavior of the coated magnesium. Appl Surf Sci. 2011;257(19):8253-7.
46. Choudhary L, Raman RKS, Nie J. In vitro evaluation of degradation of a calcium phosphate coating on a Mg–Zn–Ca alloy in a physiological environment. Corrosion. 2012;68(6):499–506.
47. Shadanbaz S et al. Growth of calcium phosphates on magnesium substrates for corrosion control in biomedical applications via immersion techniques. J Biomed Mater Res Part B Appl Biomater. 2012;101B(1):162–72.
48. Kumar M, Dasarathy H, Riley C. Electrodeposition of brushite coatings and their transformation to hydroxyapatite in aqueous solutions. J Biomed Mater Res Part A. 1999;45(4):302–10.
49. Redepenning J, et al. Characterization of electrolytically prepared brushite and hydroxyapatite coatings on orthopedic alloys. J Biomed Mater Res Part A. 1996;30(3):287–94.
50. Xie J, Riley C, Chittur K. Effect of albumin on brushite transformation to hydroxyapatite. J Biomed Mater Res. 2001;57(3):357–65.
51. Dorozhkin S, Epple M. Biological and medical significance of calcium phosphates. Angew Chem Int Ed. 2002;41(17):3130–46.
52. Kumar M, et al. Transformation of modified brushite to hydroxyapatite in aqueous solution: effects of potassium substitution. Biomaterials. 1999;20(15):1389–99.
53. LeGeros R, et al. Significance of the porosity and physical chemistry of calcium phosphate ceramics biodegradation bioresorption. Ann N Y Acad Sci. 1988;523(1):268–71.
54. Tamimi F, Sheikh Z, Barralet J. Dicalcium phosphate cements: Brushite and monetite. Acta Biomater. 2011;8(2):474–87
55. da Silva MP, et al. Transformation of monetite to hydroxyapatite in bioactive coatings on titanium. Surf Coat Technol. 2001;137(2):270–6.
56. Großardt C, et al. Passive and active in vitro resorption of calcium and magnesium phosphate cements by osteoclastic cells. Tissue Eng Part A. 2010;16(12):3687–95.
57. Tamimi F, et al. The effect of autoclaving on the physical and biological properties of dicalcium phosphate dihydrate bioceramics: brushite versus monetite. Acta Biomater. 2012;8(8):3161–9.
58. Gbureck U, et al. Resorbable dicalcium phosphate bone substitutes prepared by 3D powder printing. Adv Funct Mater. 2007;17(18):3940–5.
59. Lobovkina T, et al. Protrusive growth and periodic contractile motion in surface-adhered vesicles induced by Ca2+-gradients. Soft Matter. 2010;6(2):268–72.
60. Breitwieser GE. Extracellular calcium as an integrator of tissue function. Int J Biochem Cell Biol. 2008;40(8):1467–80.
61. Zayzafoon M. Calcium/calmodulin signaling controls osteoblast growth and differentiation. J Cell Biochem. 2005;97(1):56–70.
62. Godwin SL, Soltoff SP. Extracellular calcium and platelet-derived growth factor promote receptor-mediated chemotaxis in

osteoblasts through different signaling pathways. J Biol Chem. 1997;272(17):11307–12.
63. Titorencu I, et al. Proliferation, differentiation and characterization of osteoblasts from human BM mesenchymal cells. Cytotherapy. 2007;9(7):682–96.
64. Aguirre A, et al. Extracellular calcium modulates *In vitro* bone marrow-derived Flk-1 $^{+}$ CD34 $^{+}$ progenitor cell chemotaxis and differentiation through a calcium-sensing receptor. Biochem Biophys Res Commun. 2010;393(1):156–61.
65. Dvorak MM, et al. Physiological changes in extracellular calcium concentration directly control osteoblast function in the absence of calciotropic hormones. Proc Natl Acad Sci USA. 2004; 101(14):5140–5.
66. Dvorak MM, et al. Constitutive activity of the osteoblast Ca2+-sensing receptor promotes loss of cancellous bone. Endocrinology. 2007;148(7):3156–63.
67. Julien M, et al. Phosphate-dependent regulation of MGP in osteoblasts: role of ERK1/2 and Fra-1. J Bone Miner Res. 2009;24(11):1856–68.
68. Auer J, et al. Refining animal models in fracture research: seeking consensus in optimising both animal welfare and scientific validity for appropriate biomedical use. BMC Musculoskelet Disord. 2007;8(1):72.
69. Yamamoto A, Hiromoto S. Effect of inorganic salts, amino acids and proteins on the degradation of pure magnesium in vitro. Mater Sci Eng C. 2009;29(5):1559–68.
70. G31-72 A. Standard practice for laboratory immersion corrosion testing of metals, in materials ASfTa2004. Pennsylvania, USA.
71. Schmitz JP, Hollinger JO, Milam SB. Reconstruction of bone using calcium phosphate bone cements: a critical review. J Oral Maxillofac Surg. 1999;57(9):1122–6.
72. Fernańdez E et al. Calcium phosphate bone cements for clinical applications. Part I: solution chemistry. J Mater Sci Mater Med. 1999;10(3):169–76.
73. Knabe C, et al. Evaluation of calcium phosphates and experimental calcium phosphate bone cements using osteogenic cultures. J Biomed Mater Res. 2000;52(3):498–508.
74. Gray-Munro J, Strong M. The mechanism of deposition of calcium phosphate coatings from solution onto magnesium alloy AZ31. J Biomed Mater Res Part A. 2009;90(2):339–50.
75. Wang Y, Wei M, Gao J. Improve corrosion resistance of magnesium in simulated body fluid by dicalcium phosphate dihydrate coating. Mater Sci Eng C. 2009;29(4):1311–6.
76. Chun-Yan Z, et al. Comparison of calcium phosphate coatings on Mg–Al and Mg–Ca alloys and their corrosion behavior in Hank's solution. Surf Coat Technol. 2010;204(21):3636–40.
77. Zhang CY, et al. Preparation of calcium phosphate coatings on Mg-1.0 Ca alloy. Trans Nonferr Met Soc China. 2010;20:s655–9.
78. Li K et al. Microstructure, in vitro corrosion and cytotoxicity of Ca-P coatings on ZK60 magnesium alloy prepared by simple chemical conversion and heat treatment. J Biomater Appl. 2012;28(3):375–84.
79. Chun-Yan Z, et al. Comparison of calcium phosphate coatings on Mg–Al and Mg–Ca alloys and their corrosion behavior in Hank's solution. Surf Coat Technol. 2010;204(21–22):3636–40.
80. Xu L, Zhang E, Yang K. Phosphating treatment and corrosion properties of Mg–Mn–Zn alloy for biomedical application. J Mater Sci Mater Med. 2009;20(4):859–67.
81. Srinivasan PB, et al. Characterization of calcium containing plasma electrolytic oxidation coatings on AM50 magnesium alloy. Appl Surf Sci. 2010;256(12):4017–22.
82. Walker J et al. Magnesium alloys: predicting in vivo corrosion with in vitro immersion testing. J Biomed Mater Res Part B. 2012;100B(4):1134–41
83. Xin Y, Hu T, Chu PK. Influence of test solutions on in vitro studies of biomedical magnesium alloys. J Electrochem Soc. 2010;157(7):C238–43.
84. Witte F, et al. Biodegradable magnesium hydroxyapatite metal matrix composites. Biomaterials. 2007;28(13):2163–74.
85. Willumeit R, et al. Chemical surface alteration of biodegradable magnesium exposed to corrosion media. Acta Biomater. 2011;7(6):2704–15.
86. Kirkland N, Birbilis N, Staiger M. Assessing the corrosion of biodegradable magnesium implants—a critical review of current methodologies and their limitations. Acta Biomater. 2011;8(3): 925–36.
87. Xin Y, Hu T, Chu P. *In vitro* studies of biomedical magnesium alloys in a simulated physiological environment: a review. Acta Biomater. 2011;7(4):1452–9.
88. Yang L, et al. Effects of corrosion environment and proteins on magnesium corrosion. Corros Eng Sci Technol. 2012;47(5):335–9.
89. Chen XB, et al. In vitro corrosion survey of Mg-xCa and Mg-3Zn-yCa alloys with and without calcium phosphate conversion coatings. Corros Eng Sci Technol. 2012;47(5):365–73.